

Mass Transfer from Single Solid Spheres by Free Convection

F. H. GARNER and J. M. HOFFMAN

University of Birmingham, Edgbaston, Birmingham, England

Rates of mass transfer by free convection have been measured for spheres of three organic acids dissolving in three solvents, water, *n*-butanol and benzene. The results fell into two groups, one in which flow is completely laminar and one in which turbulence had set in in the boundary layer. Turbulence appears to set in at $N'_{Ra \text{ critical}} \sim 6 \times 10^5$.

Little work has been carried out on mass transfer by free convection from solid spheres, and usually it is treated by analogy with heat transfer. The present work was designed to measure mass transfer rates over a wide range of the relevant variables and to provide data for comparison with mass transfer at very low flow rates. A series of systems (benzoic acid in water, succinic acid in *n*-butanol, succinic acid in acetone, and salicylic acid in benzene) was chosen to give a wide variation in Schmidt and Grashof numbers.

THEORY

A dimensional analysis of the problem of mass transfer by free convection gives

$$N_{sh} = f \left[\frac{g \Delta \rho}{\nu^2 \rho}, \frac{\nu}{D} \right] \\ = f(N'_{Gr}, N'_{Sc}) \quad (1) \\ = f(N'_{Ra}, N'_{Sc})$$

Schmidt and Beckman (10) suggested that the problem could be attacked by means of boundary-layer theory. For this method to be applicable all viscous and concentration effects must be restricted to a thin layer close to the surface; that is the ratios of transverse co-ordinates and velocities to longitudinal ones are considered to be negligible ($y \ll x, v \ll u, \frac{\partial^2 u}{\partial x^2} \ll \frac{\partial^2 u}{\partial y^2}$).

Merk and Prins (9), for the case of heat transfer, show that this applies where $N_{Ra} > 10^4$. They obtained the boundary-layer equations which, written in a form applicable to mass transfer, are

$$\frac{\partial(ru)}{\partial x} + \frac{\partial(ry)}{\partial y} = 0 \\ u \frac{\partial u}{\partial x} + v \frac{\partial u}{\partial y} = g \frac{\Delta \rho}{\rho} \sin \epsilon + \nu \frac{\partial^2 u}{\partial y^2} \\ u \frac{\partial c}{\partial x} + v \frac{\partial c}{\partial y} = D \frac{\partial^2 c}{\partial y^2} \quad (2)$$

This assumes that the viscosity and diffusivity do not vary with concentration, which will be approximately true for the dissolution of sparingly soluble materials. The equivalent equations for

heat transfer are integrated to give the momentum and energy integral equations which can be solved by a method due to Squire and Eckert (13). This involves the following assumptions:

1. The thickness of the boundary layers is finite. This may be considered to be a reasonable approximation, although the real boundary layers merge asymptotically into the surrounding fluid.

2. There is negligible difference in thickness between the thermal and hydrodynamic boundary layers. This is questionable if $N_{Pr} \neq 1$, but if $N_{Pr} \gg 1$, a satisfactory agreement is obtained with Schuh's (11) more exact calculations for a flat plate.

3. Velocity and temperature profiles in the boundary layer may be represented in polynomials in y/δ .

4. The thickness of the boundary layer is small compared with the radius of curvature.

The final solution is

$$\bar{N}_{Nu} = 0.558 N_{Ra}^{1/4} (N_{Pr} \gg 1) \quad (3)$$

A parallel equation for mass transfer, with allowance for the effect of molecular diffusion, would be

$$\bar{N}_{sh} = 2.0 + 0.558 N_{Ra}^{1/4} (N_{Sc} \gg 1) \quad (4)$$

This might be expected to apply for Rayleigh numbers of 10^4 to about 10^9 , as turbulence has been found to arise in the boundary layer in experiments on heat transfer at about $Ra = 10^9$.

For turbulent free convective heat transfer in two-dimensional flow it has been shown (2) that

$$\bar{N}_{Nu} = 0.10 N_{Ra}^{0.33} \\ 2 \times 10^9 < N_{Ra} < 10^{12} \\ \text{or} \\ \bar{N}_{Nu} = 0.183 N_{Ra}^{0.81} \\ 2 \times 10^9 < N_{Ra} < 10^{15} \quad (5)$$

A parallel expression for three-dimensional flow has not been reported, but heat transfer data in this region is usually correlated by equations of the type

$$\bar{N}_{Nu} = f(N_{Ra}^{1/3}) \quad (6)$$

Some idea of the time taken for steady flow to be established may be obtained from the work of Siegel (12) who employs the method of characteristics to solve the time dependent free convection equations of momentum and energy placed in the integral form for heat transfer from a vertical flat plate. The result, written in a form applicable to mass transfer and with the assumption that $N_{Sc} \gg 1$, is

$$\frac{tD}{\bar{x}^2} = 6.5 N'_{Ra}^{-1/2} \quad (7)$$

EXPERIMENTAL METHOD

In order to obtain a large variation in Schmidt and Grashof numbers a series of systems was investigated, namely benzoic acid in water, salicylic acid in benzene, succinic acid in *n*-butanol, and succinic acid in acetone. Six different sizes of spheres were used for each system, the diameters ranging from $\frac{1}{4}$ to $\frac{7}{8}$ -in. in $\frac{1}{8}$ -in. increments. The spheres were made by compression of the crystalline acid between a punch and die in a fly-press, giving pellets of high sphericity and density.

The most important factors in the design of the apparatus were that the sphere must be held rigidly in the stagnant fluid at constant temperature, and in order to measure the rate of dissolution, photographs of the dissolving sphere must be free from distortion. A column of square cross section with plane glass windows in two opposite sides was chosen, since this would eliminate optical distortion effects arising out of the difference in refractive index between the solvent in the column and the water in the constant-temperature jacket which would enclose it. In deciding on a column 6-in. square the thickness of the boundary layer on the spheres was estimated by Merk and Prins' relationship:

$$\frac{\delta_M}{L} = \frac{x}{L N'_{Ra}}^{1/4} \quad (8)$$

It was found that the boundary layer remained thin in comparison with the clearance between the sphere and the wall for all sphere sizes over the range to be investigated, and so the walls should have little effect on the flow. Another indication is given by the work of Kraussold (6) who investigated heat transfer, for water and two oils, between two concentric vertical cylinders, the inner being heated and the outer cooled. Free convection currents were upwards at the inner cylinder and downwards at the outer. It was found that convection was suppressed and that conduction controlled for Rayleigh numbers (based on the clearance between the two cylinders) of less than 10^3 . For the systems

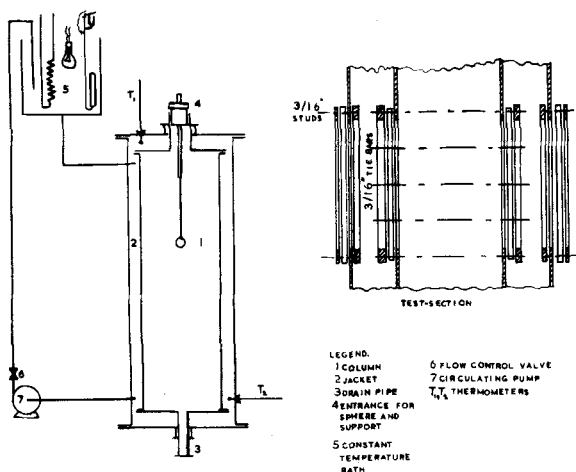


Fig. 1. Apparatus.

under investigation in the present work the Rayleigh number based on the clearance between the sphere and the walls of the column was never less than 10^{10} .

No information appears to be available for the calculation of the height of the column, so that the surfaces would have no effect on the convection currents. It was decided that for a column 3 ft. long the volume of solvent contained would be such that there would be negligible build-up in the concentration of solute around the sphere during a series of runs. Also since free convection currents should have more effect downstream than upstream, it was decided to support the spheres 1 ft. from the top of the column leaving 2 ft. clearance below them. The spheres were supported on a fine wire from the upper pole, since this was found to have negligible effect on the flow (5).

The column was completely enclosed in a constant-temperature jacket of similar construction which was designed so that water could be pumped around it rapidly from a separate constant-temperature bath without any undue pressure drop which might cause heating. The pump was mounted separately to the column on a rubber pad, and connection to the column was made with rubber tubing so that no vibrations were transmitted. The temperature in the bath was controlled by means of a 60-w. lamp, a toluene regulator, and a cooling coil, and control was generally better than $\pm 0.1^\circ\text{C}$. A diagram of the apparatus is given in Figure 1.

The column was constructed from $\frac{1}{8}$ in. thick aluminium sheeting, two pieces of which were folded until they had an L section and then welded together down the edges to give the square section required. Flanges of aluminium $\frac{3}{8}$ in. thick were welded to the top and bottom. The windows were held in place by aluminium frames connected by ten tie bars of $\frac{3}{16}$ in. diam. Cork gaskets were used as a seal. The water bath was of similar construction except that the windows were of polythene held in place by aluminium frames and $\frac{3}{16}$ in. studs. The spheres were introduced into the column through a short section of $1\frac{1}{2}$ in. diam. aluminium tubing screwed into the top end plate and which passed through a gland in the jacket. The column was drained by a $\frac{3}{8}$ -in. pipe in the bottom which also passed through a gland in the jacket. The inner column

rested on a collar which was supported by the jacket base, and the column was held in position by the friction in the glands. The sphere support consisted of 2 in. of 0.015-in. nichrome wire soldered to 7 in. of $\frac{1}{16}$ in. diam. brass rod which in turn was brazed onto 6 in. of $\frac{3}{16}$ in. diam. brass rod.

The column was supported on a framework of light angle iron with a rigid, horizontal camera platform fixed level with the front window and a 60-w. lamp illuminating an etched perspex screen fixed over the back window. The perspex screen both diffused the light and acted as a heat trap. Two thermometers 0° to 50°C . in $1/10^\circ\text{C}$. were introduced into the column through glands, one at the top and one at the bottom.

Procedure

The column was filled with the liquid under investigation and brought to constant temperature. After a period of an hour at constant temperature the sphere was introduced and its dissolution measured photographically with a speed graphic camera. This was a double extension bellows, quarter plate camera with a lens aperture of f 5.7 and a focal length of 170 mm. A supplementary lens of +3 diopters

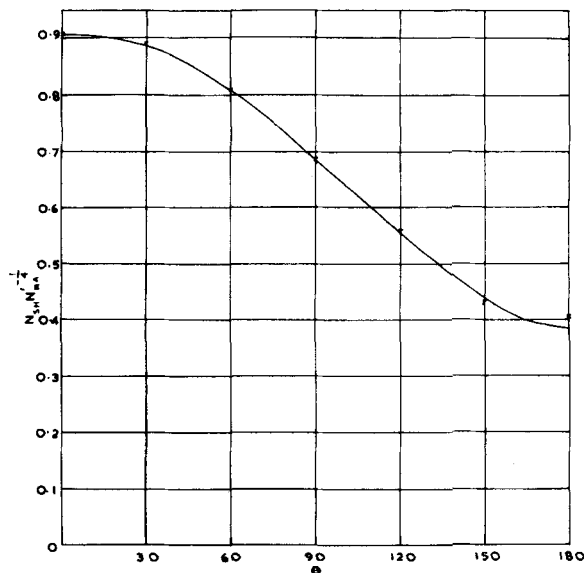


Fig. 3. Laminar free convection, local mass transfer rates.

enabled object distances as low as 5 in. to be obtained. Kodak 0-800 orthochromatic plates were used and were subsequently developed in a mixture of phenidone and hydroquinone at 70°F .

One exposure was taken at the beginning and one at the end of the test period. The negatives were projected by a diascope giving a magnification of about 20x, and the initial and final outlines of the sphere traced out. A small amount of solder on the support enabled the two silhouettes to be superimposed. The diminution of the radius at successive intervals of 10 deg. was measured around the periphery of the silhouettes. For an average diminution of radius by 0.015 in. and an over-all magnification of 20x, this diminution could be measured to within $\pm 7\%$.

Photographing the spheres in one plane only is thought to give a sufficiently accurate measure of the rate of dissolution. The spheres were of uniformly high density and care was taken to make sure that the flow was completely uniform. Thus the rate of mass transfer from the spheres should be axially symmetrical.

Mass transfer coefficients could be calculated from this diminution, h , since

$$\frac{W}{t} = \frac{h S \rho_s}{t} = K_L \cdot S \cdot \Delta c$$

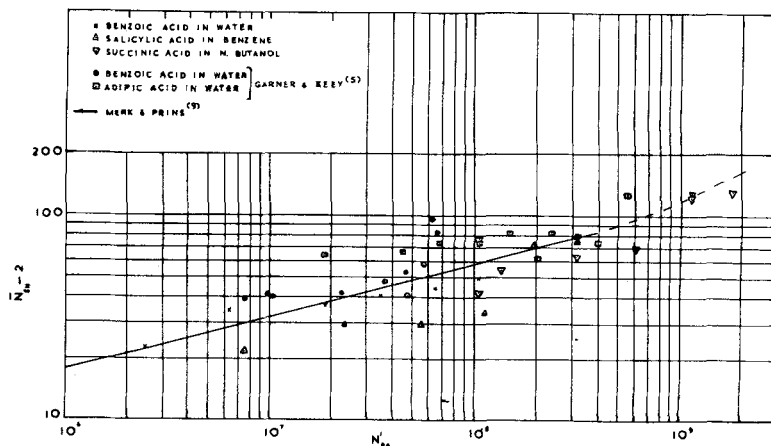


Fig. 2. Over-all transfer rates.

or

$$K_L = \frac{h \rho_s}{t \Delta c} \quad (9)$$

Over-all transfer coefficients were then calculated by finding the average dissolution, \bar{h} , by graphical integration

$$\bar{h} = \frac{\text{total volume dissolved}}{\text{surface area}} = \frac{2 \pi a^2 \int_0^\pi h \sin \theta d\theta}{4 \pi a^2} = \frac{1}{2} \int_0^\pi h \sin \theta d\theta \quad (10)$$

This photographic method of measuring mass transfer rates was chosen because it gives the variation of mass transfer over the surface of the sphere. Over-all transfer coefficients can be obtained by finding the loss of weight of the sphere over a period of time, but considerable errors can be introduced during the process of removing the solvent from the sphere before weighing.

The time for steady state to be reached was estimated by means of Equation (7) and was found to be negligible in all cases. This agrees with the work of Wilke, Tobias, and Eisenberg (15) who, in their investigation of free convective mass transfer from vertical flat plates by an electrolytical method, found the unsteady state time not to exceed a few minutes over a wide range of Rayleigh numbers.

To determine the dimensionless parameters of free convection N'_{gr} , N_{sc} , N_{sh} the following information was required: sphere density, solubility and diffusivity of the solute in the solvent, and viscosity and density of the saturated solutions.

Sphere densities were measured by Archimedes principle. The data of Gaffney and Drew (4) were used for the systems succinic acid in *n*-butanol, succinic acid in acetone, and the salicylic acid in benzene. These were all measured and should be self-consistent. The diffusivity of benzoic acid in water was estimated from the relationship of Wilke and Pin Chang (14), and the solubility was taken from the literature (1, 3). The viscosity of saturated solutions of benzoic acid in water was taken to be the same as that of pure water at the same temperature, since it is only slightly soluble. The density of saturated benzoic acid solution was measured with two 10 ml. standard graduated pycnometers, the mean of three readings with each at 30°C. being 0.99642 ± 0.00005 g./ml. All properties were evaluated at the average concentration in the boundary layer, assumed to be half the saturation value.

The total range covered is

$$2.6 \times 10^6 < N'_{Ra} < 1.8 \times 10^9$$

$$3.1 \times 10^3 < N'_{gr} < 7.7 \times 10^5$$

$$4.1 \times 10^2 < N_{sc} < 1.2 \times 10^4$$

RESULTS

The experimental results are given in the table. Those for the system succinic acid in acetone are omitted, as it was found that the rate of dissolution was too rapid. This gave severe pitting of the sphere surface and prevented accurate measurement. The over-all transfer results are plotted as $(\bar{N}_{sh} - 2.0)$ vs. N'_{Ra} in Figure 2.

DISCUSSION OF RESULTS

The results in the table fall into two separate groups, one in which the mass transfer rate is a minimum at the rear stagnation point and one in which there is a minimum elsewhere. With the latter group it has previously been shown that turbulence has set in and has resulted in the alteration of the position of the minimum (5).

Theory suggests that there is a linear relationship between N_{sh} and $N'_{Ra}^{1/4}$ for mass transfer by laminar free convection. Thus the results for the over-all transfer rate in this range were correlated by the method of least squares. The correlation coefficient was 0.795, and this was shown to be highly significant in the statistical sense. The equation of the line so obtained is

$$\bar{N}_{sh} = 5.4 + 0.440 N'_{Ra}^{1/4} \quad (11)$$

The mean error of these results is calculated as 14%; the error in projection is 7%, in diffusivity 5%, and in density 5%. Thus when one assumes these to be the major sources of error, the maximum experimental error is about 17%. There are however several points which lie outside these limits of experimental error. For the salicylic acid in benzene system this may be due to the fact that the spheres are less dense than the others, although in general the outline of the spheres after dissolution was smooth.

Nom- sphere diam., (in.)	Actual sphere diam., (in.)	Sphere density, (g./ml.)	Disso- lution time, (hr.)	Temp., (°C.)	N'_{gr}	N_{sc}	N'_{Ra}	Over-all	0°	30°	60°	90°	120°	150°	180°
Benzoic acid in water															
0.250	0.256	1.302	7.0	29.95	3.12×10^3	7.88×10^2	2.46×10^6	24.5	32.3	31.9	28.9	24.8	20.7	17.0	16.0
0.375	0.376	1.301	8.0	30.1	7.98×10^3	7.88×10^2	6.28×10^6	36.6	42.6	42.6	42.1	37.6	33.2	28.2	22.3
0.500	0.505	1.294	8.25	30.0	2.39×10^4	7.88×10^2	1.89×10^7	38.9	48.5	48.5	45.7	40.5	34.1	25.2	18.1
0.625	0.620	1.280	10.0	30.0	4.44×10^4	7.88×10^2	3.50×10^7	42.8	68.4	67.4	58.8	43.4	28.8	17.4	10.3
0.750	0.759	1.281	12.5	30.0	8.15×10^4	7.88×10^2	6.43×10^7	46.5	73.7	72.4	65.3	49.9	30.2	12.7	5.4
0.875	0.893	1.294	13.0	30.0	1.33×10^5	7.88×10^2	1.045×10^8	52.0	72.6	72.6	70.7	55.4	38.8	25.2	20.6
av: 1.292 (99.5% solid)															
Salicylic acid in benzene															
0.250	0.265	1.338	2.0	25.0	1.875×10^4	4.10×10^2	7.74×10^6	23.7	39.4	35.4	30.4	24.8	17.9	9.8	0.8
0.375	0.384	1.339	3.25	25.0	5.74×10^4	4.10×10^2	2.35×10^7	31.4	46.6	45.6	41.8	33.8	21.9	12.7	11.0
0.500	0.512	1.305	3.25	25.0	1.36×10^5	4.10×10^2	5.58×10^7	31.6	62.8	60.5	35.0	25.6	23.2	21.2	19.1
0.625	0.640	1.296	5.0	25.0	2.78×10^5	4.10×10^2	1.13×10^8	35.4	47.0	44.8	41.6	37.6	32.1	20.5	4.2
0.750	0.775	1.306	5.0	25.1	4.88×10^5	4.07×10^2	1.99×10^8	74.0	89.6	89.5	87.1	81.5	69.6	37.8	1.9
0.875	0.905	1.324	5.415	25.1	7.72×10^5	4.07×10^2	3.14×10^8	76.7	95.5	94.5	90.2	81.8	66.1	47.7	55.8
av. 1.318 (89.0% solid)															
Succinic acid in <i>n</i> -butanol															
0.250	0.262	1.509	2.25	25.0	8.46×10^3	1.22×10^4	1.035×10^8	44.5	47.2	46.8	45.7	44.2	43.3	42.3	41.3
0.375	0.383	1.495	4.0	25.0	1.14×10^4	1.22×10^4	1.39×10^8	56.2	53.0	51.4	50.6	63.0	54.6	60.2	70.6
0.500	0.499	1.497	5.25	25.0	2.58×10^4	1.22×10^4	3.14×10^8	65.4	50.5	40.0	68.9	76.0	64.1	64.1	88.7
0.625	0.619	1.508	6.5	25.0	4.95×10^4	1.22×10^4	6.02×10^8	71.0	60.0	42.2	55.5	79.4	80.5	90.1	128
0.750	0.765	1.515	6.0	25.0	9.33×10^4	1.22×10^4	1.135×10^9	131	103	104.5	134	129	112	193	249
0.750	0.764	1.514	6.25	25.05	9.33×10^4	1.22×10^4	1.135×10^9	125	103.5	101.5	126	136	123.5	134	201
0.875	0.895	1.480	6.5	25.0	1.49×10^5	1.22×10^4	1.82×10^9	133	129	103	140	140	131	143	179
av. 1.503 (96.2% solid)															

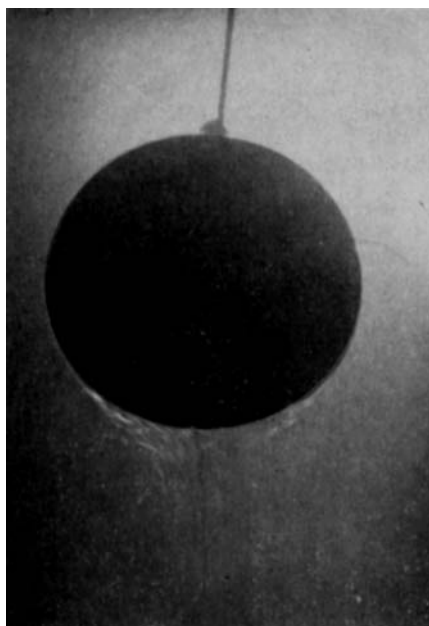


Fig. 4. Dissolving sphere showing onset of turbulence.

Equation (11) is in fair over-all agreement with Merk and Prins' theoretical equation:

$$\bar{N}_{sh} = 2.0 + 0.558 N'_{Ra}{}^{1/4}$$

but both of these are lower than Garner and Keeey's correlation (5):

$$\bar{N}_{sh} = 23.0 + 0.585 N'_{Ra}{}^{1/4}$$

In the earlier work the values used for the density of saturated solutions of benzoic acid in water differed somewhat from a value given in the literature (15), and densities were accordingly measured and found to be in good agreement with those of Wilke et al. Garner and Keeey's results, recalculated on this basis, are shown in Figure 2 together with the present work; the former are still somewhat higher than the latter. This may be due to improved temperature control in the present work eliminating thermal convective currents. However it can be seen that both sets of results can be correlated by the equation of Merk and Prins with a mean deviation of about $\pm 25\%$. The large scatter may be due to the fact that the experiments were performed on the threshold of turbulence. If flashes of turbulence, such as those observed in cylindrical pipes (7), occurred, the rate of transfer would be increased.

The results for the local mass transfer rates are more scattered than those for the over-all transfer. This is to be expected, since the former will be more affected by any error in superimposing the two sphere outlines prior to measurement. Thus it is thought that the best way to represent local transfer rates for laminar free convection is to plot $N_{sh} N'_{Ra}{}^{-1/4}$ vs. θ , since it has been

shown theoretically that the product $N_{sh} N'_{Ra}{}^{-1/4}$ is almost independent of N'_{Ra} for $N_{sc} \gg 1$ (9). When one assumes this product to be constant at a given point on the sphere surface, the mean probable errors of the average local transfer rates at successive angles of 30 deg. beginning at the front pole for the present work together with that of Garner and Keeey are $\pm 22.4, 20.0, 21.5, 20.2, 22.9, 31.0$, and 39.6%. These errors, with the exception of the last two, are of the same order as the experimental error, and the large deviation is not surprising near the rear pole where the transfer is low and difficult to measure with any accuracy.

The local mass transfer rates for laminar free convection are presented in Figure 3. These are somewhat higher than those predicted for heat transfer (9), but over most of the surface of the sphere (up to $\theta = 140$ deg.) the form of the distribution is in good agreement. Disagreement near the rear pole is to be expected, since in this region the boundary layer thickens rapidly and the flow leaves the sphere in the form of a tail; therefore boundary-layer theory will no longer apply. It is probable that towards the rear of the sphere the velocity gradient will increase, since fluid will be falling almost vertically away from the sphere. This would tend to counteract the thickening of the boundary layer and result in transfer tending to remain constant near the rear pole, as is shown by the experimental results:

The variation of mass transfer rate around the surface of the sphere tends to be rather undulating for turbulent flow. This may be caused by flashes of turbulence similar to those which have been found in transitional flow in circular pipes before the motion becomes fully turbulent (7). Such flashes would increase the mass transfer rate locally.

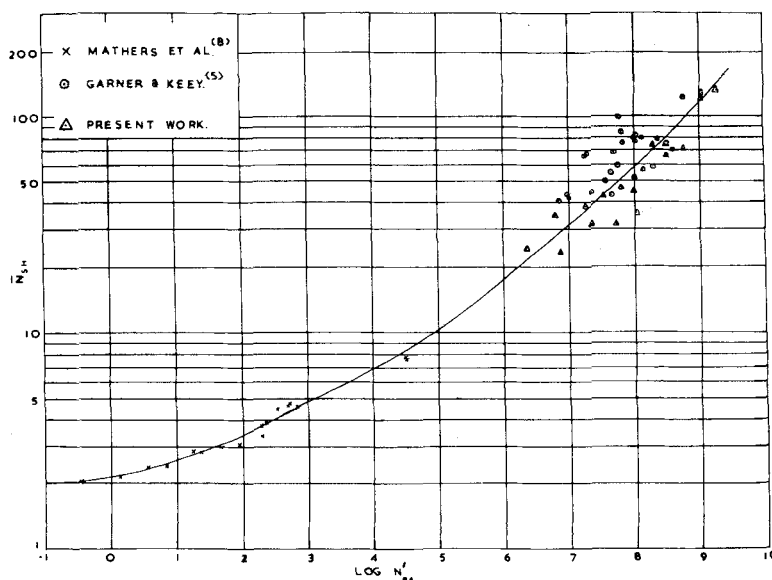


Fig. 5. Isothermal mass transfer by free convection.

It is thus difficult to state exactly when turbulence sets in, but the results suggest a critical Rayleigh number of from 2 to 6×10^8 , based on the distance along the sphere surface from the front pole to the point of onset of turbulence. This may be compared with a value of 3.5×10^8 obtained by Garner and Keeey (5).

Figure 4 clearly shows the onset of turbulence in the boundary layer. This is a photograph of a benzoic acid sphere dissolving in acetone. The solubility is high, and the boundary layer is visible because of the variation of refractive index with concentration. The thin streak of light around the surface of the sphere down to an angle of about 150 deg. from the front stagnation point is the laminar boundary layer. Near the bottom of the sphere the boundary layer thickens rapidly, and the flashes of light show that turbulence has set in. The flow leaves the sphere in a characteristic tail.

The points obtained in the turbulent region are few and scattered, but the dotted line has been drawn through them. Its slope changes from one quarter in the laminar region to one third as required by theory. More experimental work is needed to position this line accurately.

These results are compared with data on the sublimation of naphthalene and benzene coated spheres at low pressures (8) in Figure 5. The latter cover a much lower Rayleigh number range than the present work, but the two sets of data seem to be consistent.

NOTATION

- a = sphere radius, L
- c = concentration, ML^{-3}
- d = sphere diameter, L
- D = diffusivity, L^2T^{-1}
- f = functional sign, —

g = gravitational acceleration, LT^{-2}
 h = diminution of radius, L
 K_L = mass transfer coefficient, LT^{-2}
 L = characteristic length, L
 r = distance radially from sphere center, L
 S = surface area, L^2
 t = time interval, T
 u = velocity parallel to surface, LT^{-1}
 v = velocity normal to surface, LT^{-1}
 W = total mass transferred, M
 x = distance coordinate along surface, L
 y = distance coordinated normal to surface, L

Greek Letters

δ = boundary-layer thickness, L
 θ = angle from forward stagnation point
 ϵ = angle between normal to surface and the vertical
 ν = kinematic viscosity

ρ = density (fluid)
 ρ_s = density (solid)

Dimensionless Groups

$N_{Gr} = g d^3 \beta \Delta T / \nu^2$ = Grashof number
 $N'_{Gr} = g d^3 \Delta \rho / \nu^2 \rho$ = modified Grashof number for mass transfer
 $N_{Nu} = h d / D$ = Nusselt number
 $N_{Pr} = \nu / K$ = Prandtl number
 $N_{Ra} = g d^3 \beta \Delta T / \nu K$ = Rayleigh number
 $N'_{Ra} = g d^3 \Delta \rho / \nu^2 \rho \cdot \nu / D$ = modified Rayleigh number for mass transfer
 $N_{Sc} = \nu / D$ = Schmidt number
 $N_{Sh} = K_L d / D$ = Sherwood number

LITERATURE CITED

1. Anttane, E. C., and T. F. Doumani, *Ind. Eng. Chem.*, **41**, 2015 (1949).
2. Bayley, F. J., *Proc. Inst. Mech. Eng.*, **169**, 361 (1955).
3. Bourgoïn, R., *Ann. chim. et phys.*, **15**, 161 (1878).
4. Gaffney, B. J., and T. B. Drew, *Ind. Eng. Chem.*, **42** (1), 1120 (1950).

5. Garner, F. H., and R. B. Keey, *Chem. Eng. Sci.*, **9**, 218 (1958).
6. Kraussold, Hermann, *Forsch. Gebiete Ing.*, **5**, 186 (1934).
7. Lindgren, E. R., *Arkiv. Für Fysik*, **7**, 23, (1954).
8. Mathers, W. G., A. J. Madden, and E. L. Piret, *Ind. Eng. Chem.*, **49**, (6), 961 (1957).
9. Merk, H. J., and J. A. Prins, *Appl. Sci. Res.*, **A**, 4, 11 (1953-54).
10. Schmidt, E., and W. Beckman, *Tech. Mech. u. Thermodyn.*, **1**, 391 (1936).
11. Schuh, H., "Temperaturgrenschichten," Göttinger Monographien, B6 (1946).
12. Siegel, Robert, *Trans. Am. Inst. Mech. Engrs.*, **80**, 2, 347 (1958).
13. Squire, H. B., and E. R. G. Eckert, in "Modern Developments in Fluid Dynamics," Oxford Univ. Press, England (1938).
14. Wilke, C. R., and Pin Chang, *A.I.Ch.E. Journal*, **1**, 264 (1955).
15. Wilke, C. R., C. W. Tobias, and Morris Eisenberg, *Chem. Eng. Progr.*, **49**, 663 (1953).

Manuscript received September 9, 1959; revision received April 27, 1960; paper accepted April 28, 1960.

The Distribution of Nitric Acid Between Water and Tributyl Phosphate - Hexane Solvents

DONALD R. OLANDER, LUCIEN DONADIEU, and MANSON BENEDICT

Massachusetts Institute of Technology, Cambridge, Massachusetts

The distribution of nitric acid between water and solutions of tributyl phosphate in n-hexane has been measured over a greater range of acid and tributylphosphate concentrations than have been reported previously.

The partitioning of nitric acid between water and tributylphosphate-hexane solvents has been satisfactorily explained on the basis of the commonly accepted equilibrium complexing reaction, with this modification: The over-all aqueous-to-organic reaction is subdivided into the distribution of uncomplexed nitric acid and an organic phase complexing reaction. This alteration is found necessary to account for the behavior of the partitioning data of dilute acid over the entire tributylphosphate-hexane range. The residual discrepancy between the theory and the data can be qualitatively attributed either to modest nonideality of the organic phase or to the effect of the varying water content of the solvent on the distribution coefficient of uncomplexed nitric acid.

The sparse data on water extraction by tributylphosphate-hexane solvents are not amenable to the same type of analysis, even though a type of complexing similar to that found for nitric acid has been previously proposed. The interaction between water and tributylphosphate appears to be stronger than that normally attributed to nonideality but weaker than a true chemical complex.

Like many heavy metal nitrates nitric acid reacts chemically with tributylphosphate to form a stable complex. Although the compound nitric acid-tributylphosphate has never been chemically isolated, its existence has been conclusively demonstrated by the ultraviolet spectral evidence of Collopy and Blum (3). However no ana-

lytical method has yet been devised to differentiate quantitatively the small amount of physically dissolved nitric acid from the complex in the organic phase.

Warf (13) and Moore (11) were the first to point out the competitive effect of nitric acid on the extraction of the lanthanide and actinide nitrates. Alcock (1), Fletcher (4), and Gruverman (6) have done further experimen-

tal work on the extraction of pure aqueous nitric acid into tributylphosphate, while Kooi (7) and Fletcher (4) have investigated the partitioning of nitric acid between water and other organic solvents. Recently Alcock et al. (1), McKay and Healy (10) and Tuck (12) have subjected the nitric acid-water-tributylphosphate diluent system to an exhaustive examination. An excellent summary of the physical chemistry of these complexing reactions has been presented by Glueckauf (5), while Baldwin et al. (2) have investigated the distribution of a large number of monovalent electrolytes between water and tributylphosphate.

Nitric acid, unlike the heavy metal nitrates, does not have a coordination number to be fulfilled; yet there is strong evidence that it forms only one complex with tributylphosphate, namely nitric acid-tributylphosphate. First the spectrum of nitric acid tributylphosphate solutions indicates no higher complexes (3). Secondly there is a tendency for the organic phase to saturate at a 1-to-1 mole ratio of nitric

Donald R. Olander is at The University of California, Berkeley, California.